Title
Sound wall barriers: Near roadway dispersion under neutrally stratified boundary layer

Authors
Pournazeri, Sam
Princevac, Marko

Publication Date
2015-12-01

DOI
10.1016/j.trd.2015.09.025

Peer reviewed

Transportation Research Part D 41 (2015) 386–400

Contents lists available at ScienceDirect

Transportation Research Part D

journal homepage: www.elsevier.com/locate/trd

Sound wall barriers: Near roadway dispersion under neutrally stratified boundary layer

Sam Pournazeri, Marko Princevac *

Department of Mechanical Engineering, University of California Riverside, Riverside, CA 92521, United States

ARTICLE INFO

Keywords:
Air quality
Dispersion
Roadside structures
Roadway emissions
Sound barriers
Water channel

ABSTRACT

With the passage of California Senate Bill 375, which motivates infill development near transit hubs, there is the potential to increase vehicle congestion in residential communities and increase in human exposure to toxic mobile source pollutants. Among all the mitigation strategies that protect near roadway residents from health-affecting vehicular emissions (e.g. separating sensitive receptors from high traffic roadways), this paper discusses the impact of sound wall barriers (SBs) in reducing the air pollution exposure of nearby residents. To date, there have been some studies done to understand the impact of these structures on dispersion of vehicular emissions; however, no definitive conclusion has been drawn yet. The main objective of this paper is to provide more information and details on flow and dispersion affected by barriers through a systematic laboratory simulation of plume dispersion using a water channel. Three sets of experiments were conducted: (1) plume visualizations, (2) plume concentration measurements, and (3) flow velocity measurements. Results from this study shows that the deployment of sound barriers induces a recirculating flow over the roadway which transports the surface released emissions to the upwind side of the roadway, and then shifts the plume upward through an induced updraft motion. Plume visualizations clearly demonstrate that the presence of SBs induce significant vertical mixing and updraft motion on the roadway which increases the initial plume dilution and plume height and consequently results in reduced downwind ground level concentrations. Although different SB configurations result in different localized flow patterns, the dispersion pattern does not change significantly after several SB heights downwind of the roadway.

Introduction

Numerous epidemiological studies have shown that long-term exposure to outdoor air pollution increases the risk of respiratory diseases, birth defects, premature mortality, cardiovascular disease, and cancer (Dockery and Pope, 1994; Harrison et al., 1999; Wilhelm and Ritz, 2003; Peters et al., 2004; Jerrett et al., 2005; McConnell et al., 2006). Houston et al. (2006) showed that more than 24,000 childcare centers in California are within 200 m of highly trafficked roadways with more than 50,000 vehicles per day. A statistical analysis has shown that children diagnosed with asthma are more likely to live within 500 m of major roadways (Edwards et al., 1994).

* Corresponding author.
E-mail address: marko@engr.ucr.edu (M. Princevac).

http://dx.doi.org/10.1016/j.trd.2015.09.025
1361-9209/

As part of the California climate action goals to reduce greenhouse gas (GHG) emissions (Assembly Bill 32; http://www.arb.ca.gov/cc/ab32/ab32.htm), the California Air Resources Board has adopted a land-use reform called SB375 (http://www.arb.ca.gov/cc/sb375/sb375.htm), which is a landmark legislation that aligns regional land use, transportation, housing, and greenhouse gas reduction planning efforts. This legislation requires the Metropolitan Planning Organizations to prepare sustainable community strategies to reduce the miles traveled by passenger vehicles with the goal of reducing the GHG emissions. Following this land-use reform, there is a potential to increase in the number of people living near high traffic roadways. Although California state law restricts the siting of new schools within 500 feet of a highly trafficked freeways and urban roads (http://www.arb.ca.gov/ch/handbook.pdf), there is no such requirement on residential communities. Therefore, air quality agencies are looking for other mitigation options to avoid the possible increase in the near-roadway exposure due to implementation of SB375. One of these strategies that has recently received more attention are roadside structures.

Although the primary purpose of roadside structures, such as sound barriers (SBs) and vegetation is to reduce noise, they can have a significant impact on the dispersion of pollutants by enhancing the turbulent mixing and raising pollutants further from the ground level. In addition, roadside vegetation can improve air quality by removing and filtering particulate matter and increasing the deposition of heavy metals (Beckett et al., 1998; Bowker et al., 2007; Brantley et al., 2014). Numerous field (Veranth et al., 2003; Bouvet et al., 2007; Pardyjak et al., 2008; Finn et al., 2010; Mao et al., 2013), wind tunnel (Heist et al., 2009) and numerical studies (Bowker et al., 2007; Steffens et al., 2013; Speckart and Pardyjak, 2014) have been conducted to address the impact of SBs and surrounding vegetation on the dispersion of traffic related emissions. It has been shown that for low wind speed and stable atmospheric condition, SBs can trap pollutants on the upwind side, increasing on-road pollutant concentrations (Finn et al., 2010; Baldauf et al., 2008). Baldauf et al. (2008) also showed that due to the finite length of the SBs some pollutants may be channeled into the leeward region of the SB, increasing the ground-level concentrations downwind of the barrier. The *Near Roadway Tracer Study* (NRTS08) conducted at Idaho Falls, Idaho by the National Oceanic and Atmospheric Administration (NOAA) shows that a concentration decrease of up to 50% compared with an unobstructed roadway can be achieved with different roadway configurations (Clawson et al., 2009; Finn et al., 2010). The results also indicate that increasing the atmospheric stability can reduce the effectiveness of SBs by increasing ground-level concentrations.

The effect of roadway elevation relative to the surrounding terrain has been investigated in the US Environmental Protection Agency wind tunnel (Heist et al., 2009). It has been shown that the smallest reduction in ground-level concentration occurs for elevated roadways and the maximum decrease happens in the case of depressed roadway with SBs on the sides. Bussoti et al. (1995) showed that broadleaves and small needle conifers are the most efficient species for eliminating heavy metal particles by enhancing deposition and preventing them from being transported farther downwind. Results from the model by Bowker et al. (2007) reveal that the presence of both SBs and vegetation can significantly reduce the concentration downwind by producing more turbulence and mixing. The study also stated that, with the presence of SBs, a more uniform and vertically well mixed plume can be observed (Bowker et al., 2007).

Most of the above-mentioned studies are more focused on the overall impact of SBs in reducing the ground level concentrations and do not sufficiently describe how these structures modify dispersion in terms of flow and turbulence. A thorough understanding on the direct impact of SBs on flow and dispersion can significantly help air quality modelers in development of dispersion models that can accurately predict the human exposure in the areas close to highways. Furthermore, most of these studies do not describe the impact of SBs under wind directions other than perpendicular to the SBs. Non-perpendicular wind directions can induce channeling between the SBs, which may be important in transferring most pollutants to less sensitive areas in order to decrease human exposures. Clawson et al. (2009) was one of the very few studies that investigated the impact of sound barriers under non-perpendicular approach flows; however, this study was only focusing on a single barrier configuration, which is not capable of generating channeling flow. Heist et al. (2009) investigated limited configurations that were all dominated by recirculating flow between the SBs, and only a perpendicular wind direction was investigated. Note that the simple model utilized by Heist et al. (2009) cannot reproduce channeling.

The present study aims to delineate the effects of various SB configurations on near-roadway dispersion through systematic water channel simulations. Laboratory simulations for dispersion of vehicular emission in the presence of SBs are investigated through (1) plume visualization and (2) concentration measurements. These results are accompanied with detailed flow measurements, which are needed to interpret the visualized plume patterns and measured ground level concentrations. The experimental setup and measurement techniques are described in Section 'Laboratory setup'. Section 'Laboratory experiments' presents results from all tested configurations. Visualization results are in Section 'Plume visualization', followed by concentration measurements in Section 'Concentration measurements' and velocity measurements in Section 'Velocity measurement'. Summary and conclusions are given in Section 'Summary and conclusion'.

Laboratory setup

Water channel

The water channel has a test section that is 1.5 m long, 1 m wide and 0.5 m deep. Water is circulated through the channel test section using a 20 HP axial pump (Carry Manufacture, Inc), which can produce a maximum mean velocity of 0.5 m s^{-1} in the test section. Velocity is controlled through a variable frequency controller with a resolution of 1/100 Hz. Flow conditioning is achieved with profiled honeycombs and custom-built perforated screens. The perforated screens are used to generate desired inflow velocity profiles as part of the flow conditioning. The channel has flow control capability to maintain a desired velocity profile starting from the classical logarithmic to the linear profile. Experiments presented in this paper are all with the logarithmic mean velocity profile. Profiles of the mean horizontal (v) and vertical (w) velocities together with their standard deviations (v_{rms} and w_{rms}) are shown in Fig. 1. It can be seen that the vertical profile of horizontal wind speed is highly similar to logarithmic wind profile especially for heights up to 100 mm. Vertical profiles of standard deviation of horizontal and vertical velocities are maintained constant with a slight peak at 2.5 cm from the ground. The reference Reynolds number, based on the free stream velocity (v_∞) and characteristics length scale, H_b^* (length scale based on the obstacle frontal area; $H_b^* = (WH)^{1/2}$) was Re = 12,600, which is sufficient to satisfy Reynolds number independency criteria of $Re \approx 4000$ (Halitsky, 1968; Fackrell and Pearce, 1981; Snyder, 1981; Yee et al., 2006). Although, such high Reynolds number satisfies the conditions to simulate real world atmospheric dispersion in the water channels, it needs to be noted that due to the nature of laboratory flow simulation systems, flows in water channels are more coherent than real atmosphere.

The water channel is equipped with a Particle Image Velocimetry (PIV) system for velocity measurements. Detailed velocity fields can be measured in the vertical or horizontal plane. This typically involves producing a pair of laser pulses, which are recorded onto a pair of camera frames. The frames are then split in a large number of interrogation areas, often called tiles. It is then possible to calculate a displacement vector for each tile using image processing. This is converted to a velocity using the time between consecutive images (in our case Δt = 1.5 ms). The PIV measurement technique is well established and widely used for fluid flow investigations (Adrian, 1988, 1991, 1997; Prasad et al., 1992) and will not be discussed here in detail. More details on the water channel facility can be found in Pournazeri et al. (2010).

Fluorescent dye, Uranine, is used as the tracer dye for flow visualizations as it has high light intensity in the range of visible light. Uranine has a very low molecular diffusivity; hence, the corresponding Schmidt number ($Sc = v/D$ where D is the diffusivity of Uranine in water; and v is the kinematic viscosity of water) is relatively large ($Sc \sim 2000$). Since typical Reynolds numbers for the present case are quite high, turbulence will be the leading mechanism in dispersing the tracer dye, and the molecular diffusivity will serve as a smoothing mechanism for small-scale concentration discontinuities (Snyder, 1972). Therefore, due to the turbulent nature of the flow, matching Sc to the field is not required. Images of the dyed plume were captured using long exposure imaging (30 s). This technique gives us averaged plume behavior, which is used to understand dispersion under different flow conditions and sound barrier configurations. More details on flow visualization can be found in Pournazeri et al. (2012a).

Simulating flow and dispersion in such a laboratory facility requires utilizing correct scaling techniques. These scaling methods are explained in detail by Pournazeri et al. (2012b) and will not be repeated here.

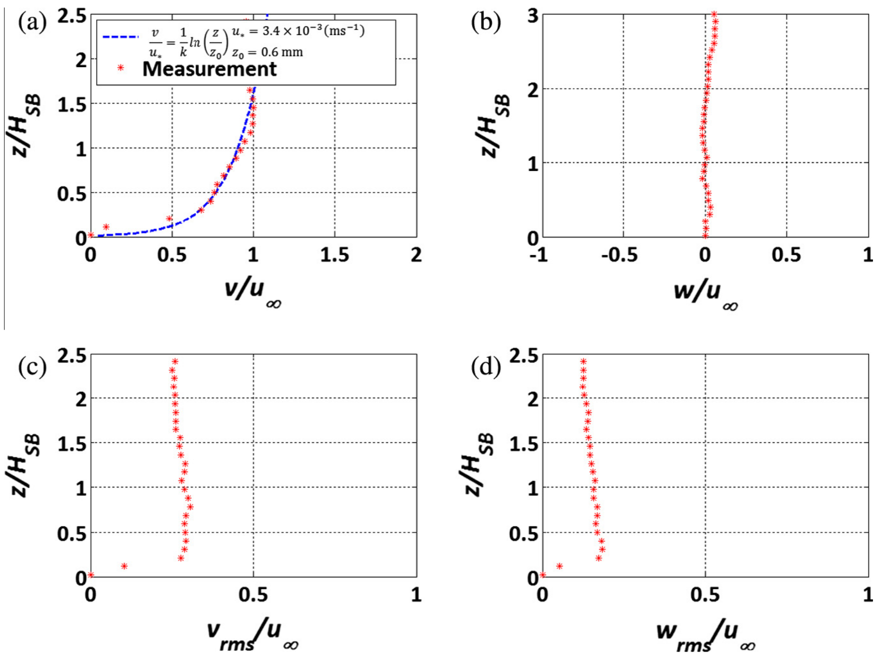

Fig. 1. Profiles of ambient mean (a) horizontal v (m s^{-1}) and (b) vertical w (m s^{-1}) velocities and standard deviations of (c) horizontal v_{rms} (m s^{-1}) and (d) vertical w_{rms} (m s^{-1}) velocities. Dashed blue line represents the logarithmic wind profile. Vertical distance z and velocities are normalized with respect to sound barrier height H_{SB} = 0.08 m and free stream horizontal velocity (v_∞ = 0.045 m s^{-1}). (For interpretation of the references to color in this figure legend, the reader is referred to the web version of this article.)

Concentration measurements system

The Fiber Optic Assisted Laser Induced Fluorescence (FOALIF) system consists of a 400 mJ Nd-YAG laser (Big Sky Laser Technologies Inc.), which produces a 532 nm wavelength laser beam with the frequency of up to 15 Hz, a laser pulse synchronizer (TSI Inc.), a high resolution (1600×1192) POWERVIEW 2 M CCD camera (TSI Inc.), and a 575–585 nm light filter. The basic operating principal of FOALIF is as follows: the laser beam expands through a cylindrical lens into a laser sheet and enters the fiber optic bundle. Next, the laser light is carried via the emitting fibers to the sensors, which are placed at desired locations in the water channel. The emitting fibers at the sensors will illuminate any dye that is in the vicinity and the dye will fluoresce. The fluorescent light, as well as residual light from the laser, is captured by the receiving fibers. The light captured by the receiving fibers is sent through a filter so that only the desired fluorescent light is captured and recorded by the CCD camera. The intensity of this captured light is proportional to the concentration as shown by Guilbault (1973). For these set of experiments, concentrations were sampled for 300 s under 1 Hz sampling rate. Further information on the setup, basic theory and operation of FOALIF can be found in Pournazeri et al. (2013).

A solution of Rhodamine in water (60 mg L^{-1}) was pumped through a line source at a rate of 3.87 mL s^{-1}. LEGO type blocks were used to construct the SBs in the channel and they spanned the whole width of the channel to simulate infinite SBs. The water channel models are geometrically scaled by 100 relative to the field size. The road width was chosen as 30 cm (30 m scaled to the field) and a finite line source of 20 cm (20 m scaled to the field) was placed in the center of the roadway. All FOALIF experiments were done with an incoming logarithmic velocity profile with friction velocity of $u_* = 0.34$ (cms^{-1}), roughness length of $z_0 = 0.6$ mm, and a free stream velocity of 4.2 cm s^{-1} (4.2 m s^{-1} scaled to the field) at 10 cm from the ground. Details of scaling of flow and dispersion in the water channel are provided in Pournazeri et al. (2012b).

Laboratory experiments

Many different SB configurations were studied through plume visualizations while only selected cases were further investigated through concentration measurements. Hence, the initial round of experiments solely focused on visualizations of the plume behavior under different geometrical and meteorological conditions.

Plume visualization

For the plume visualization experiments, each SB configuration includes three line sources, one for each pair of lanes (assuming a 6-lane highway). The Initial road model configurations include: (1) No SB, (2) equal height SBs, (3) only upwind SB, (4) only downwind SB, (5) upwind barrier of double height, and (6) downwind barrier of double height. The impact of wind direction (0°, 30°, and 60°) as well as the effects of terrain elevation (raised and sunken roadways) were also studied, but only for the configurations of no SBs and SBs of equal height ($H_{up} = H_{down}$). All experimental parameters are summarized in Table 1.

Impact of barrier configuration

Visualization results from different SB configuration are shown in Fig. 2. As can be seen, SBs lead to larger vertical dispersion of pollutants. This increase in vertical dispersion occurs as a result of the recirculating flow between the SBs which creates the updraft next to the upwind barrier and also induces higher turbulence levels. The comparison between different configurations shows that for the case of double SBs and upwind SB, the average behavior of the plume does not change significantly. Unlike the case with double SBs, when only the downwind SB is present, the size of the recirculating flow is limited by the height of the barrier rather than the width of the roadway. Therefore, the recirculating flow is expanding across a

Table 1
Experimental parameters covered in the plume visualization experiments.

Parameter	Values	
Barrier heights	Walls of equal height Upwind wall of double height	Downwind wall of double height
Wind speed	Low flow rate, corresponding to 3 m s^{-1} Moderate flow rate, corresponding to 4.5 m s^{-1}	High flow rate, corresponding to 8 m s^{-1}
Wind direction	Perpendicular to the wall, $\alpha = 0^o$ $\alpha = 30^o$	$\alpha = 60^o$
Release buoyancy	Light release, SG = 0.98 Neutral release, SG = 1.00	Heavy release, SG = 1.02
Surrounding vegetation	No vegetation Mature trees	Mature trees in combination with SBs
Road height	In level with surrounding terrain Sunken	Raised

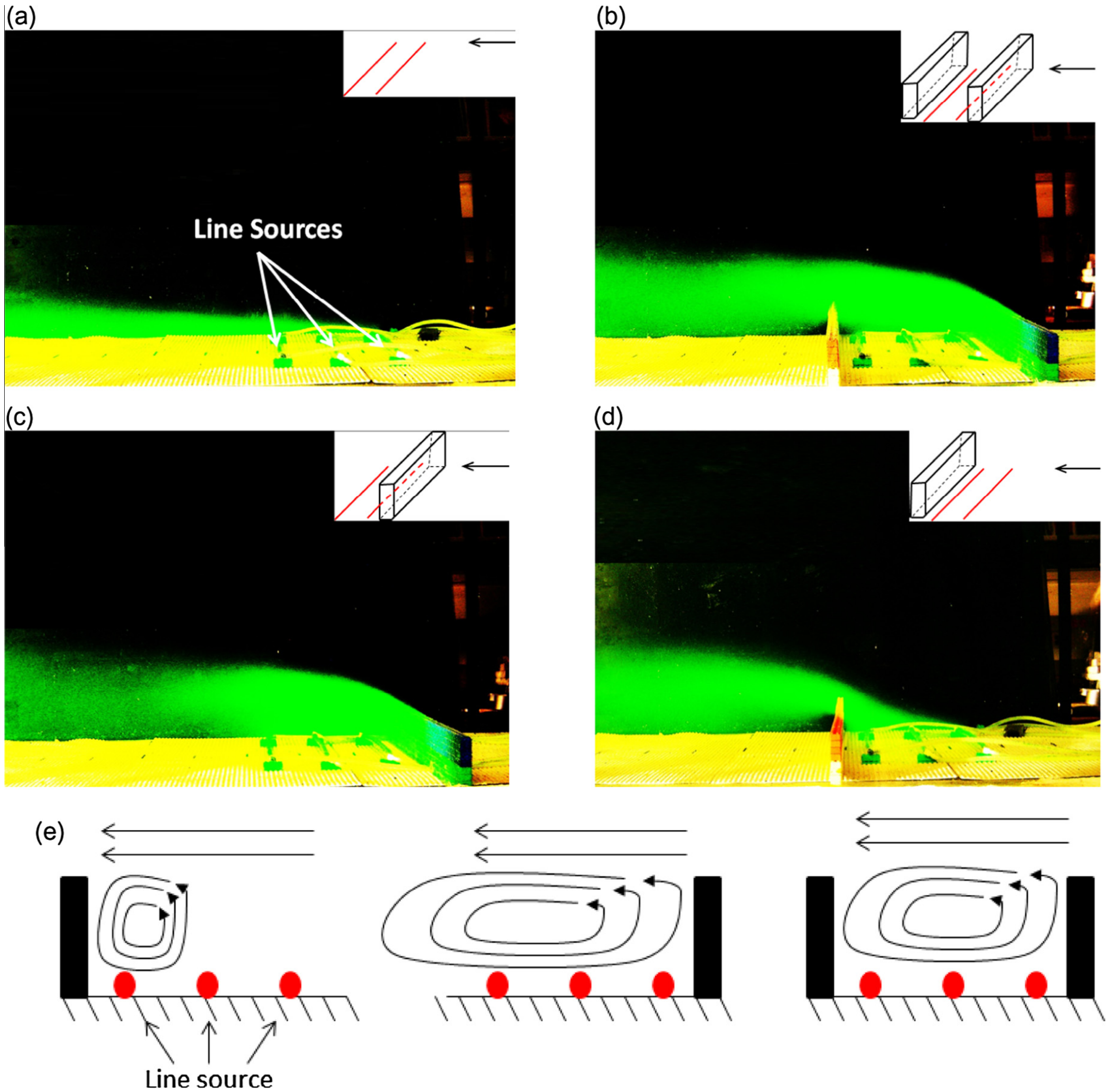

Fig. 2. Plume visualization for (a) without; and with (b) double, (c) upwind, and (d) downwind SBs. Arrow on the schematic presents the flow direction. (e) Schematic of the change in the size of recirculation flow under different sound barrier configurations.

smaller region of the roadway as compared to the double SBs and upwind SB cases. Snyder and Lawson (1994) have also reported similar results through their wind tunnel experiments around building obstacles. As a result of such flow conditions, for the case of downwind SB, the plume (i.e. vehicular emissions) will be impacted by the high-turbulent region (i.e. recirculating flow) within a shorter travel distance; and will not disperse as much as in the case with double SBs. Therefore, one should expect higher on-road concentrations for the case of only downwind SB compared to the other two cases (double SBs and upwind SB only). Fig. 2e shows a schematic of the change in the size of the recirculation flow under different sound barrier configurations.

Impact of barrier heights

Fig. 3 shows the results of plume visualization with SBs of unequal height ($H_{up} \neq H_{down}$). In this case, the initial height of the barriers is chosen to be 4 cm (equivalent to 4 m in the field) whereas in the previous case (Section 'Impact of barrier configuration'), the barrier heights were 8 cm (equivalent to 8 m in the field). As can be seen from Fig. 3, increasing the height of the upwind SB results in larger vertical plume spread. However, increasing the height of the downwind SB does not change the plume spread significantly compared to the case with equal SB's heights. The results from this experiment also show that the vertical plume spread is directly proportional to the height of the SB. This is important for dispersion modeling since it

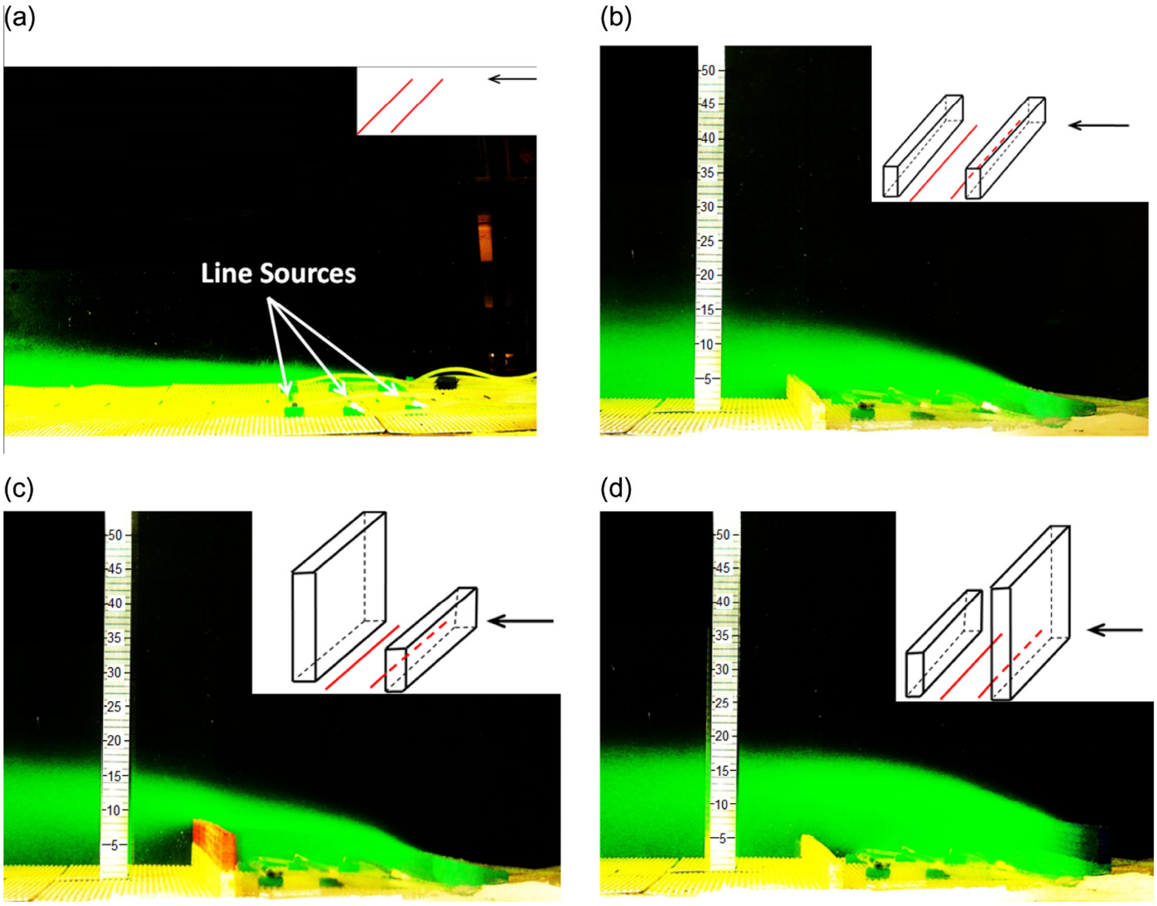

Fig. 3. Plume visualization for (a) without; and with (b) walls of equal height (H_{SB} = 4 cm) (c) downwind wall of double height (H_{down} = 8 cm) (d) upwind wall of double height (H_{up} = 8 cm).

directly determines the length scale associated with the initial vertical spread of the plume. As in the case of single SB, the upwind SB is more effective in lifting the plume due to the strong recirculation in the wake of the SB (flow field measurements are given in Section 'Velocity measurement'). Similar observations are also reported in Addepalli and Pardyjak (2013) for flow characteristics in the step-up/down street canyons.

Impact of wind direction

The effect of SBs on the vertical spread of plume under different wind directions of $\alpha = 0°$ (wind direction perpendicular to SB), $\alpha = 30°$, and $\alpha = 60°$, were investigated (Fig. 4). For this specific case, sound barrier lengths were selected to be less than 1/2 of the width of the water channel to avoid the impact of the walls on the flow that is channeled between the two barriers. Results from this series of plume visualizations reveal that the average behavior of the plume significantly changes when the wind direction shifts from $\alpha = 0°$ to $\alpha = 60°$. As the wind angle increases, the flow pattern changes from recirculating flow to channeling flow and this leads to flushing of pollutants along the roadway, which may lead to higher on-road concentrations.

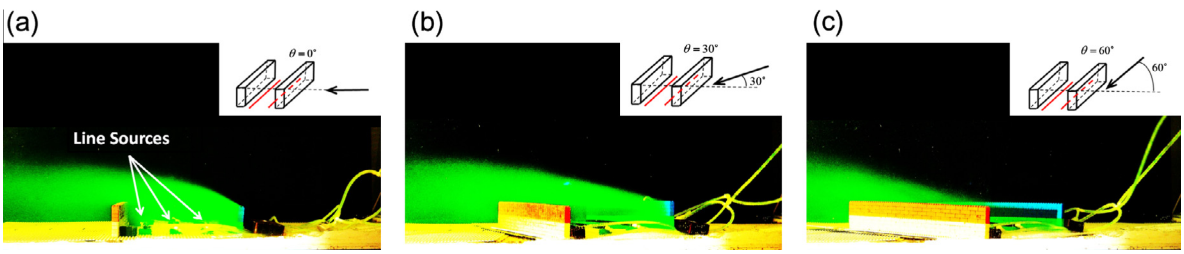

Fig. 4. Plume visualization for different wind angles of (a) $\alpha = 0°$ (b) $\alpha = 30°$ (c) $\alpha = 60°$ SBs of finite length (L = 50 cm).

This effect will be analyzed further through the velocity measurements shown in Fig. 13. The channeling of flow through the roadway (between the SBs) also changes the pattern of the plume's vertical spread from the one proportional to the square root of distance from the source to a more linear growth with distance. As incident flow angle increases from 0° to 60°, the effect of the SB on the vertical spread of the plume is reduced; and the dispersion becomes more dominated by flow channeling rather than recirculating flow. As compared to the case with flow approaching perpendicular to the sound barriers, vertical spread of the plume is smaller under non-perpendicular wind directions due to lower turbulence levels.

Sunken and raised roadways

This study also investigated the influence of terrain elevation on the dispersion of roadway emissions under two different terrain categories of (1) sunken and (2) raised roadways.

Raised roadways. As it can be seen from the results (Fig. 5), raised roadways increase the plume height, which decrease the ground level concentrations in short distances from the roadway accordingly. Since our problem is involved with surface releases, this fact can be translated into lower maximum ground level concentrations. The presence of SBs at the same level as the roadway substantially increases the vertical spread as well as the initial dilution. These two complementary effects (raised plume due to the terrain and the initial dilution caused by SBs) can significantly reduce the ground level concentrations. However, in the case where no SBs are present, Fig. 5a shows that the plume is descending toward the ground at some distances downwind of the roadway. A raised roadway modifies the flow and causes a downdraft downwind of the roadway. This downdraft can bring the plume down and hence, reduce the effectiveness of raised roadways in surface level concentration reduction. This effect will be further discussed in Section 'Velocity measurement'.

Sunken roadways. The impact of sunken roadways was also studied under three different barrier configurations: (1) no SBs (Fig. 6a), (2) the barriers located on the flat terrain above highway (Fig. 6b) and (3) barriers located at the same level of highway (Fig. 6c). Results from these experiments reveal that sunken roadways without any barriers (Fig. 6a) does not enhance the vertical spread of the plume substantially and the plume mostly follows the terrain pattern, however, the raised SBs (Fig. 6b) significantly increases the plume spread by transporting the plume to the upwind side of the roadway. The reason for this behavior is that in the presence of raised SBs and sunken roadway, a strong recirculating flow is induced in the region between two SBs, which enhances the mixing of pollutants and increases the vertical spread of the plume within a relatively larger region as compared to the sunken SBs. In the case where SBs are located at the same level as the roadway (Fig. 6c), due to low approaching wind speed, this recirculating flow is relatively weaker; thus lower mixing occurs and plume spread does not increase significantly. Therefore, as compared to other cases (Fig. 6a and c), lower surface level concentrations are expected under the raised SBs configuration (Fig. 6b).

Concentration measurements

In addition to plume visualizations, which provide a qualitative understanding, quantitative ground level concentrations for selected SB configurations were also measured. The FOALIF experiments were performed for the roadway configurations of no SB, upwind only SB, downwind only SB, $H_{up} = H_{down}$, $H_{up} = 2H_{down}$, and $H_{down} = 2H_{up}$. Fig. 7 shows schematics of the tested configurations. Results from the concentration measurements are shown in Fig. 8. Results are presented in terms of normalized concentration versus normalized downwind distance (X/H_{SB} where X is the downwind distance and H_{SB} is the height of the SB). Normalized concentration is defined as

$$\chi = \frac{C\ U\ L_x\ L_y}{Q} \quad (1)$$

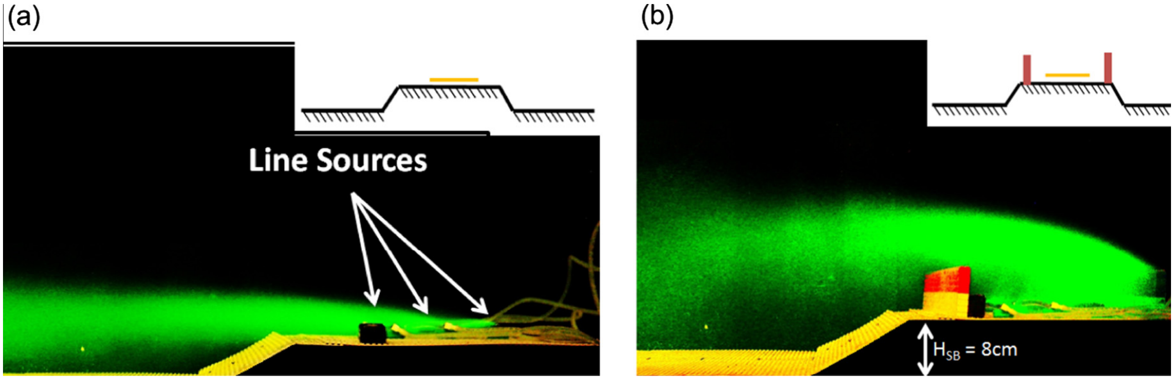

Fig. 5. Plume visualizations under raised roadway condition with (a) no SB and (b) raised SBs.

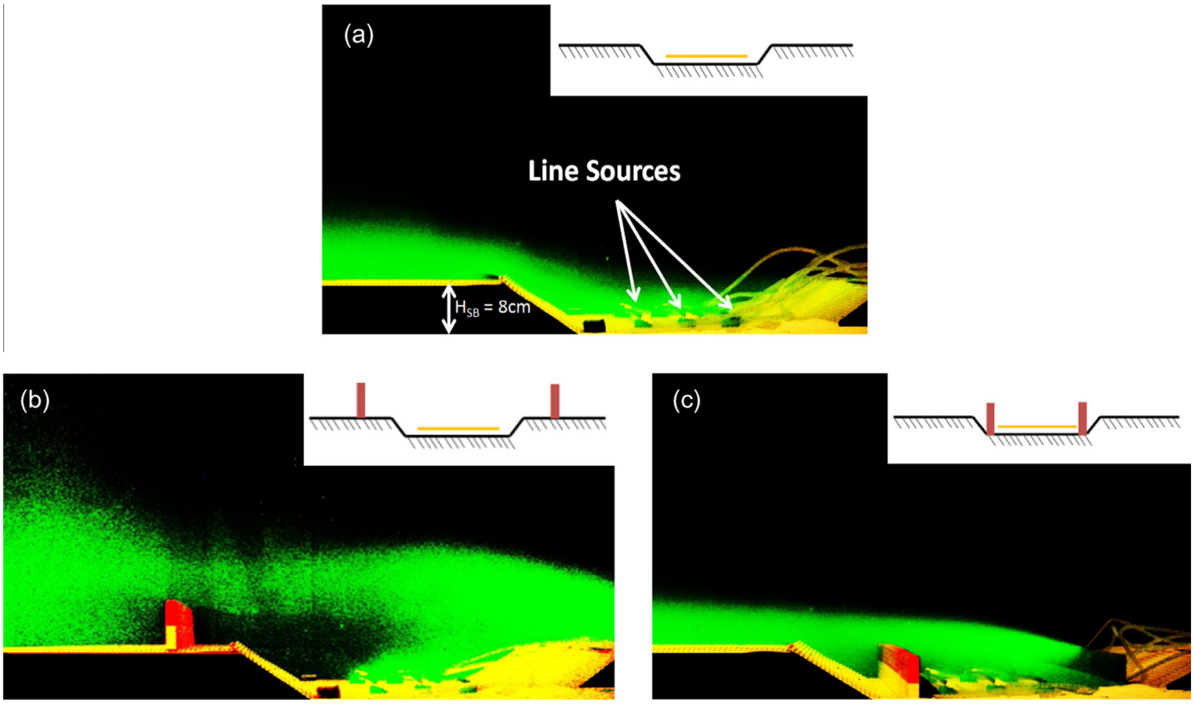

Fig. 6. Plume visualization for different SB configuration under sunken roadway condition. (a) No SB (b) raised SBs, and (c) sunken SBs.

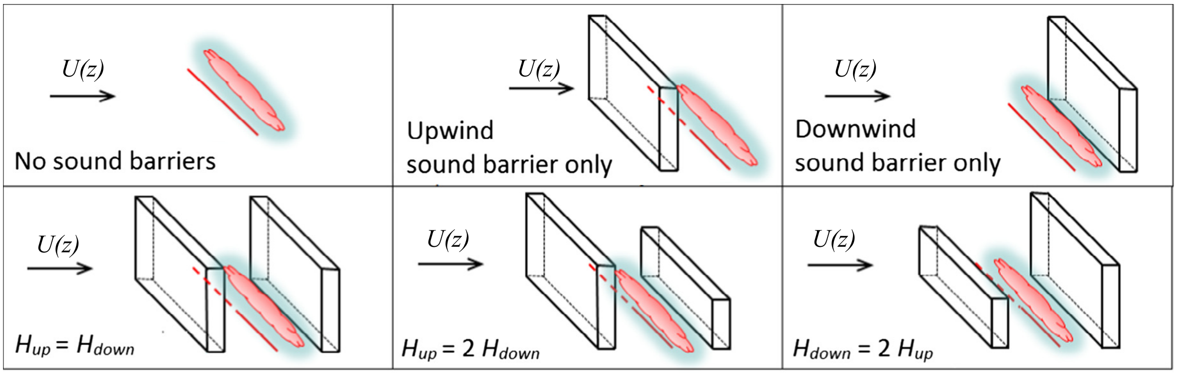

Fig. 7. Tested configurations for concentration measurements.

where C (kg m^{-3}) is the concentration, U (m s^{-1}) is the mean velocity, Q (kg s^{-1}) is the emission rate of the line source, L_x (m) and L_y (m) are horizontal and lateral length scales. L_x and L_y were chosen as the road width and source length respectively. Although it is common to normalize the concentration results for the case of no SBs based by the friction velocity and roughness length, in order to have consistency for each roadway configuration, the case of no SB was normalized in the same way using Eq. (1).

Similar to the results obtained in the previous section, concentration results also confirm that the presence of SBs decreases the ground level concentration downwind of the barriers. Results also show that further downwind of the barriers, the ground level concentrations for different SB configurations become very similar; however, different levels of on-road ground level concentrations can be seen. Although enhanced turbulence within the SBs increases the vertical spread of the plume and causes a reduction in on-road ground level concentrations, the dominating recirculation flow in this region will substantially increase the residence time of the pollutants and may adversely increase the ground level concentrations. These two effects counteract each other in increasing or decreasing the on-road concentrations and prevent unexpected changes of on-road pollutant exposure. Among all the configurations, the highest on-road concentration is associated with the case where height of the upwind SB is double the height of the downwind SB. This maximum concentration occurs upwind of the source. Due to the strong recirculating flow associated with the wake of upwind SB, emissions from the

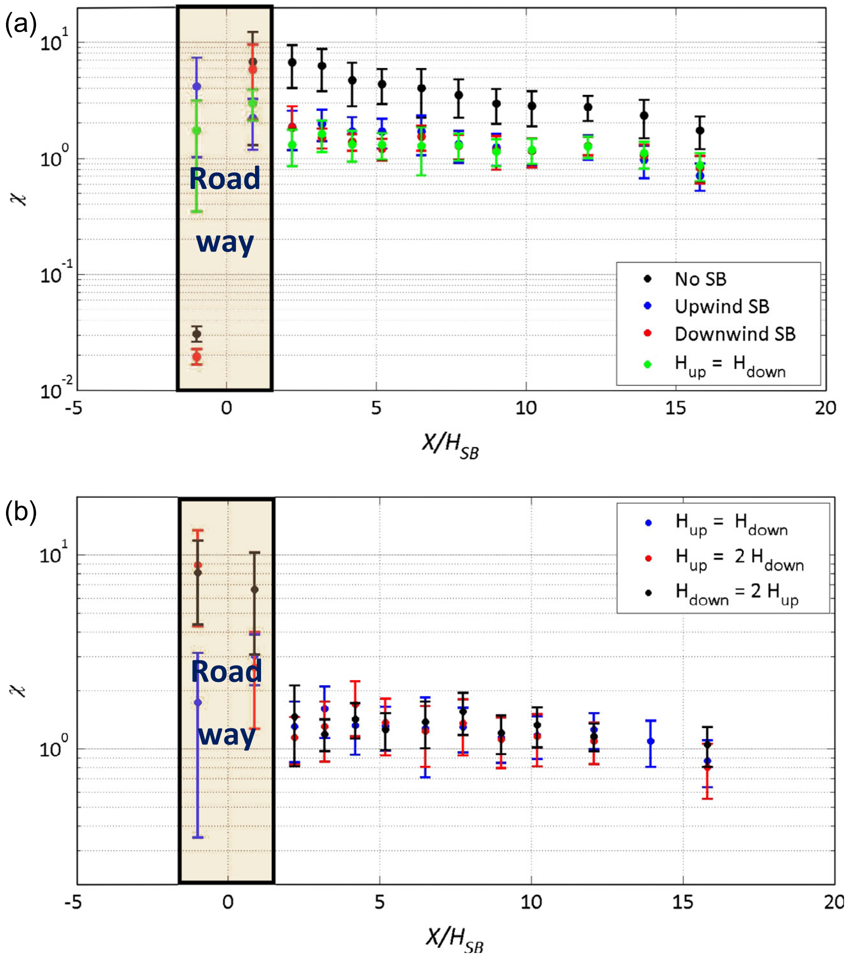

Fig. 8. Ground level concentration measurements for (a) different SB configuration (b) different SB height ratio (H_{up}/H_{down}). The center of the roadway is located at $x = 0$. Error bars represents standard deviation of concentrations from the average.

sources travels upwind with relatively low velocity and gets advected up at the upwind barrier. This causes high ground level concentrations upwind of the source. However, downwind of the source, the maximum on-road concentration is associated with the cases where only a downwind SB is present and the case where height of the downwind SB is double the height of the upwind SB ($H_{down} = 2H_{up}$). In these two cases, pollutants get trapped in the wake cavity produced by the downwind SB on the windward side. In addition, due to the lower vertical spread of the plume above the SB, high concentration pollutants will be trapped and hence, higher ground level concentrations can be observed on the leeward of the downwind barrier. In the case where only a downwind SB is present, the ground level concentration on the upwind side of the roadway becomes minimal since there is no mechanism to direct the pollutants toward that side. This correlates well with the visualizations (Fig. 2d) which show almost no plume upwind of the emission sources. For the roadway configuration of $H_{down} = 2H_{up}$, there is a recirculating flow which brings pollutants back toward the upwind barrier where they are advected up and this increases the on-road concentrations near the upwind side of the roadway (Fig. 8b). This is also confirmed through the plume visualizations shown in Fig. 3c. The results from the case where only the downwind SB is present follows a similar pattern as that shown in Finn et al. (2010), where concentrations downwind of the barrier were measured under neutral stability conditions in the Idaho Falls field study. In comparison to the Idaho Falls field data (Finn et al., 2010), concentrations in the water channel decrease slower. The main reason for this effect is the limited crosswind dispersion imposed by the side-walls of the water channel that do not allow the concentrations to decrease rapidly at relatively far distances from the source (e.g. in this case it is $x \approx 15\ H_{SB}$ where x is the distance from the center of the roadway).

Velocity measurement

In order to better interpret the dispersion process of pollutants released from roadways under different SB configurations, the results from plume visualization and concentration measurements are supplemented with velocity measurements. PIV measurements were done for the same SB and roadway configurations as the plume visualization experiments. Flow measurement results for each configuration are explained next. Please note that due to the pixel light saturation or decreased intensity of laser light at certain locations, a very few number of vectors shown in the figures associated with the velocity measurement are not representing the actual flow field and should be disregarded.

Single SB and SBs of equal height

Flow for four different configurations were measured: (1) no SBs (2) double SB; (3) downwind only SB; and (4) upwind only SB. Results from these measurements are all shown in Fig. 9. The flow measurements from this study reveal that the main impact of SBs on the wind flow is the generation of a recirculating flow over the roadway, which enhances the turbulence and mixing. Such enhancement in turbulence was also confirmed through our measurements of horizontal and vertical velocity fluctuations (in case with SBs, the root mean squared of velocity fluctuations is higher). However, the size of this recirculating flow is significantly dependent on the configuration of SBs as similarly shown by Snyder and Lawson (1994). In the case of double SBs (Fig. 9b), the size of this recirculating flow is constrained to the width of the roadway; however, in the absence of the downwind SB (upwind SB only), this recirculating flow becomes much larger and in the absence of upwind SB it becomes smaller. The size and the strength of this recirculating flow play major roles in the mixing of the vehicular emissions from the roadway as described in Section 'Impact of barrier configuration'.

SBs of unequal height

Fig. 10 shows the results of flow measurement under different SB height ratio (H_{up}/H_{down}). For the case where the upwind SB is double the height of the downwind SB, the recirculating flow is smaller than that of the isolated upwind SB case (Fig. 9d), however, it is still larger than the case where downwind SB is double the height of upwind SB. As it was explained earlier in Section 'Plume visualization', these differences might yield different dispersion patterns leading to different ground level concentrations in close vicinity of SBs. The stronger the recirculating flow is, the higher the initial dilution would be, and hence lower ground level concentration will be observed.

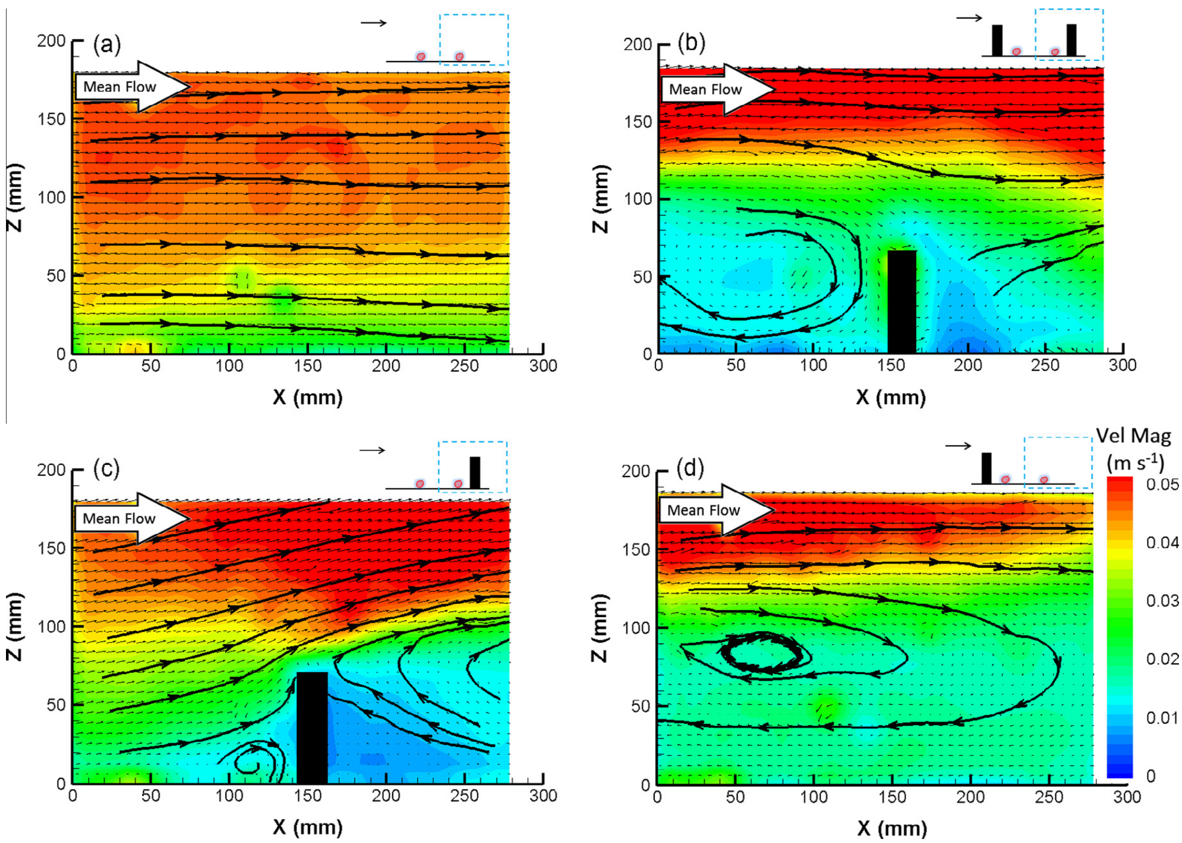

Fig. 9. Velocity measurements for (a) no SB, (b) double, (c) downwind only, and (d) upwind only SB configuration. For each measurement, 300 PIV images were captured at a sampling rate of 1 Hz. The box with the blue dashed line in the inset represents the location of velocity measurements (i.e. PIV frame). (For interpretation of the references to color in this figure legend, the reader is referred to the web version of this article.)

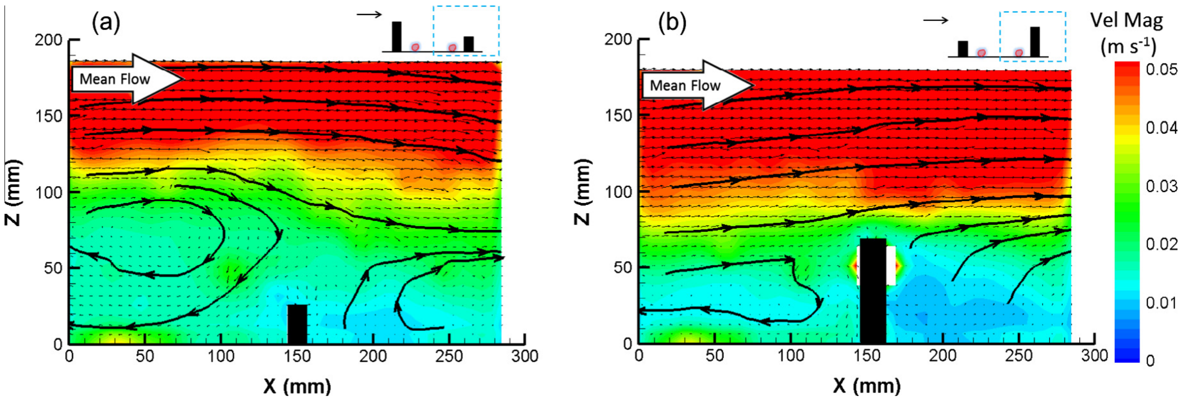

Fig. 10. Velocity measurements for (a) upwind SB of double height and (b) downwind SB of double height. For each measurement, 300 PIV images were captured at a sampling rate of 1 Hz. The box with the blue dashed line in the inset represents the location of velocity measurements (i.e. PIV frame). (For interpretation of the references to color in this figure legend, the reader is referred to the web version of this article.)

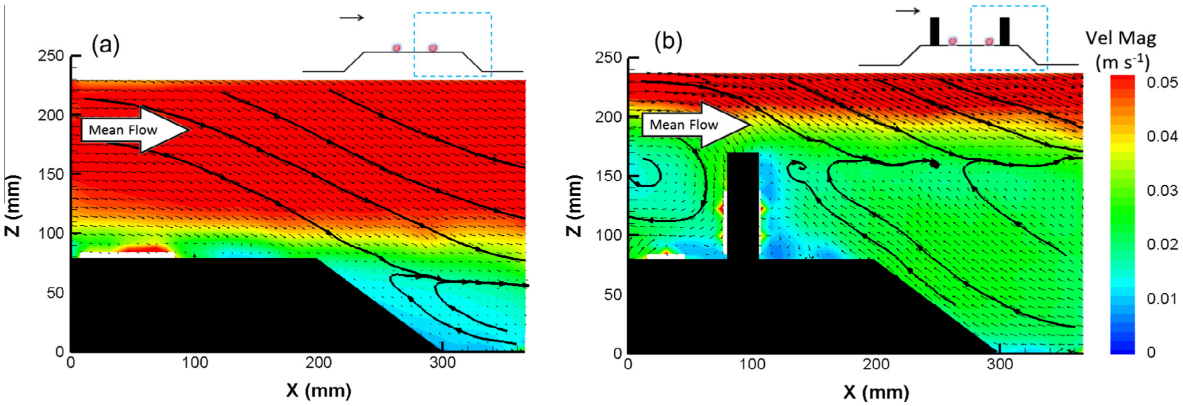

Fig. 11. Velocity measurement for raised roadway (a) with no SBs (b) in the presence of raised double SBs. For each measurement, 300 PIV images were captured at a sampling rate of 1 Hz. The box with the blue dashed line in the inset represents the location of velocity measurements (i.e. PIV frame). (For interpretation of the references to color in this figure legend, the reader is referred to the web version of this article.)

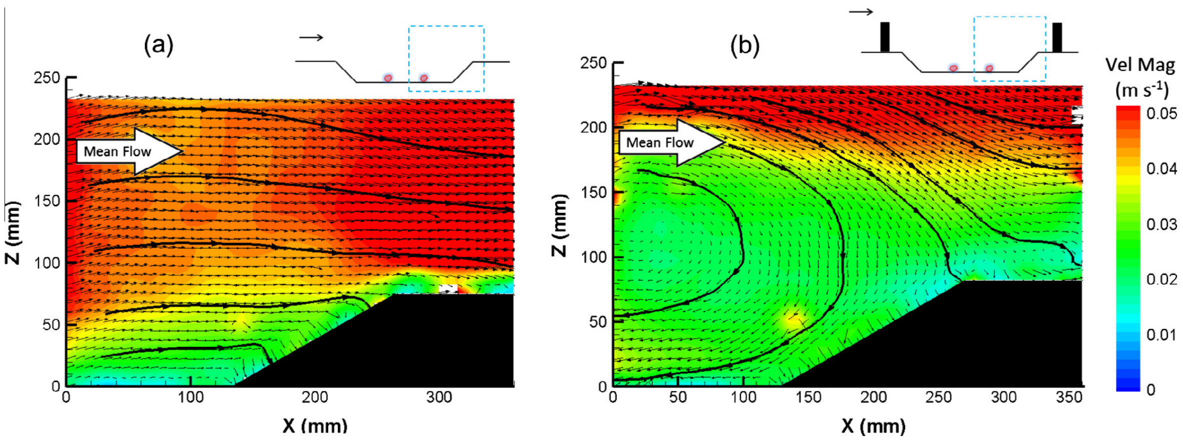

Fig. 12. Velocity measurement under sunken roadway (a) with no SBs and (b) in the presence of double SBs. For each measurement, 300 PIV images were captured at a sampling rate of 1 Hz. The box with the blue dashed line in the inset represents the location of velocity measurements (i.e. PIV frame). (For interpretation of the references to color in this figure legend, the reader is referred to the web version of this article.)

Sunken and raised roadways

Velocity measurements were also conducted for two different roadway configurations: (i) raised and (ii) sunken roadways.

Raised roadways. As was shown earlier in Section 'Sunken and raised roadways', raised roadways can decrease the ground level concentrations by elevating the plume downwind of the roadway. However, the incorporation of raised roadways changes the mean flow, which can accordingly modify the dispersion pattern. Therefore, it is necessary to understand the

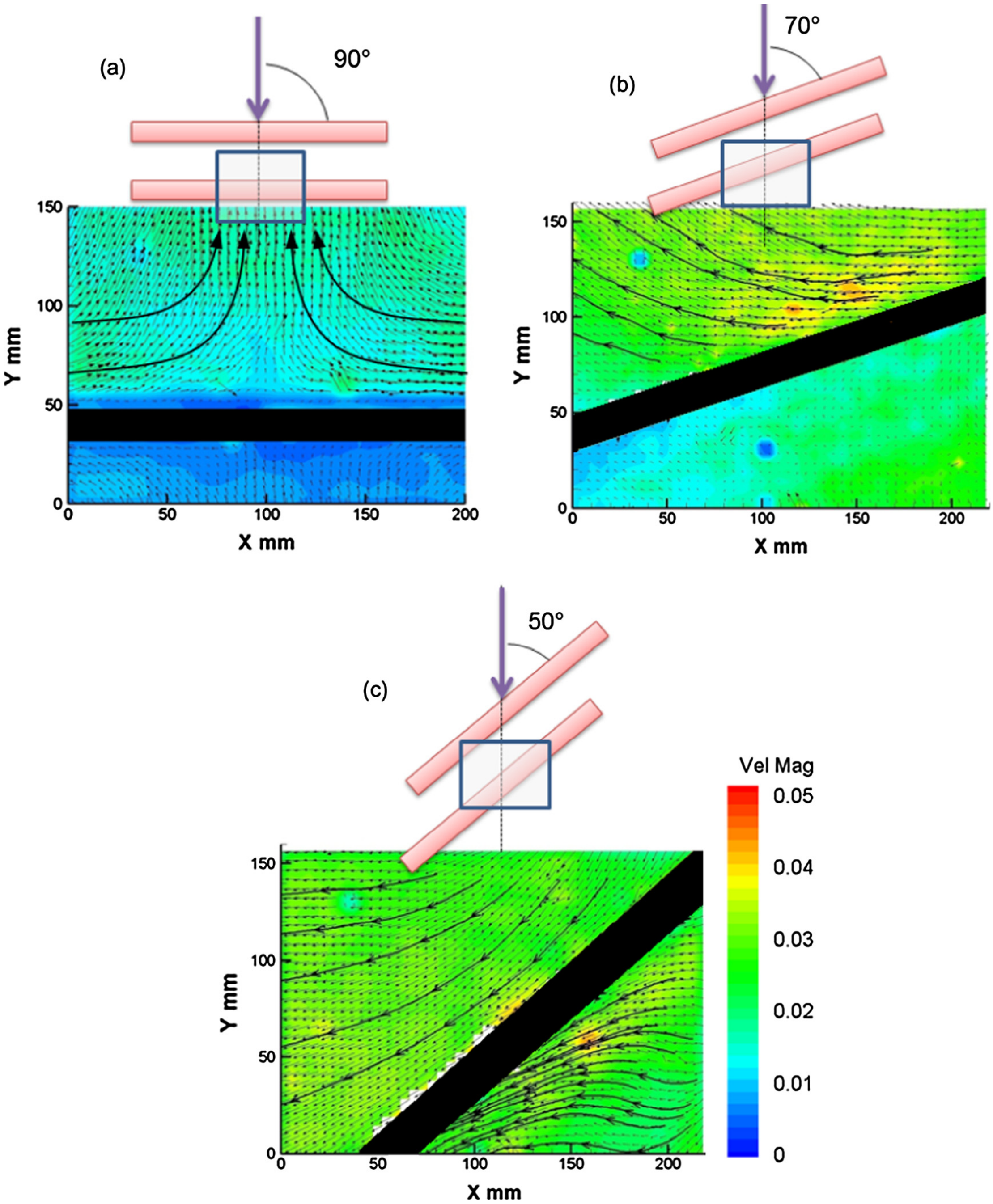

Fig. 13. Velocity measurement at different wind directions of (a) $\theta = 90°$, (b) $\theta = 70°$ and (c) $\theta = 50°$. For each measurement, 300 PIV images were captured at a sampling rate of 1 Hz. The box with the blue dashed line in the inset represents the location of velocity measurements (i.e. PIV frame). (For interpretation of the references to color in this figure legend, the reader is referred to the web version of this article.)

flow modification under such configurations. Fig. 11 shows the results from flow measurements under raised roadway configurations with and without the presence of SBs.

As it can be seen in Fig. 11a, raised roadways induce strong downdrafts ($w/U_\infty \approx 0.45$) downwind of the roadway and cause the plume to descend more toward the ground. As also discussed by Heist et al. (2009), this phenomena may reduce the efficacy of raised roadways in ground level exposure reduction. As shown by Fig. 11b, the incorporation of SBs on the raised roadways modifies the flow significantly, as it reduces the downdraft in the immediate vicinity of the roadway and produces a recirculating flow between the SBs which enhances the dispersion of vehicular emission.

Sunken roadways. The effect of sunken roadways on the flow was also investigated under two different SB configurations (Fig. 12). For the case of no SB the flow follows the terrain with lower velocities on the roadway (Fig. 12a). Since no recirculating flow is formed, relatively high initial dilution of plume is not expected and this effect combined with low wind speeds on the roadway may increase the on-road concentrations. The inclusion of SBs produces recirculation over the roadway (Fig. 12b) with relatively lower near surface velocity due to the depressed terrain. This large recirculation area results in greater on-road vertical spread of the plume (i.e. dilution) which can further decrease the ground level concentrations downwind as compared to the flat roadway. This is also consistent with the results reported by Heist et al. (2009).

Wind direction

One of the significant effects of SBs on the flow and dispersion of roadway emissions is the development of channeling flow which occurs when the incoming wind is not perpendicular to the roadway. This effect has been studied by Princevac et al. (2010) through urban arrays, and it was shown that the strength of this channeling flow is highly dependent on the inhomogeneity of tall buildings in urban areas. In this study, the occurrence of along the road channeling under different wind directions is investigated by measuring the horizontal flow fields (Fig. 13).

As can be seen in Fig. 13, in the case where wind direction is perpendicular to SBs, two counter-rotating vortices develop between the SBs as well as downwind of the SBs. Changing the wind direction by 20° (20° increment was chosen due to the limitation of the PIV experimental setup; these limitations did not exist for plume visualizations), changes the flow structure completely and flow channeling occurs between the SBs. By increasing the wind direction to 40°, the channeling becomes uniform and the flow direction becomes parallel to barriers. This flow can significantly change the dispersion of roadway emissions. In such conditions, vehicular emissions travel along the roadway with limited horizontal spread due to the presence of SBs. The vertical spread of the plume is also driven by the upwind flow turbulence only. Under such dispersion conditions, relatively high on-road concentration levels are expected.

Summary and conclusion

Vehicular emissions are known to be one of the major sources of air pollution in cities. The negative air quality impacts of these pollutants effect people living in close proximity of highways and major roadways. Therefore, in the past 30 years, many studies focused on the dispersion of emissions from traffic inside urban areas. Most of these studies simulated roadways as line sources located on the ground with no major structure in the vicinity. However, since the mid-20th century, major highways have commonly been surrounded with wall-like structures known as SBs. These structures are mainly designed to protect residential areas close to the highway from the noise pollution. However, the effectiveness of these structures on reducing the air pollution from highways has not been sufficiently explored. Hence, in this study, we explained how various SB configurations effect pollutant dispersion through a series of laboratory experiments conducted in the water channel. These experiments mainly consisted of plume visualizations and selected concentration measurements, along with velocity measurements. From the plume visualizations, it was shown that SBs increase the vertical spread of the plume, and that different configurations of SBs yield similar vertical spread downwind of the roadway. It has also been shown that increasing the height of the barriers increases the initial vertical spread of the plume proportionally. Although the increase in the vertical spread of the plume results in lower concentrations downwind of the roadway, the recirculating flow generated by the presence of the sound barrier transport the plume upwind and increase the concentrations upwind of the source. During these experiments, we also investigated impact of the terrain configuration (sunken vs. raised roadways) on the dispersion patterns. The results indicate that sunken roadways with barriers located above the roadway, yield to the maximum mixing and presumably the lowest downwind concentrations, but potentially higher upwind concentrations.

Concentrations downwind of SBs were measured using the newly developed concentration measurement system. It has been observed that different SB configurations (upwind, downwind and double SBs) yield similar concentration patterns downwind of the SBs, which confirms our earlier observations through the plume visualizations under the same configurations. However, the concentration measurements showed that these different configurations lead to different on-road concentrations, which can vary up to a factor of 10 (mainly on the upwind of the source).

Flow measurements show that the major flow pattern governing the mixing of pollutants within barriers is the recirculating flow which occurs as a result of the cavity produced by the barriers. The size of this recirculating flow can vary substantially under different configurations. However, measurements under different wind directions showed that the recirculating flow diminishes rapidly as the wind direction deviates from normal. It has been observed that when the wind direction changes from normal, the flow channels between the barriers. This channeling flow can transport the vehicular emissions along the roadway and substantially increases the on-road ground level concentrations. Under such circumstances, the presence of SBs can also substantially contribute to the increase in the on-road ground level concentrations since they inhibit the lateral spread of the plume.

In conclusion, results from this study shows that roadside structures such as SBs, reduce both on-road as well as downwind ground level concentrations by enhancing the mixing of the pollutants and elevating the plume by a length-scale proportional to the barrier heights. This effect can be weakened when the wind direction changes from normal to the SBs. Terrain can be considered as an additional mitigation option to increase the initial dispersion of the plume and hence reducing the concentrations. It needs to be noted that results presented in this paper are based on the assumption that vehicular emissions are released near the surface (~0.5 m above the ground) and cannot be extrapolated to the cases where exhaust tailpipe is 3–4 m above the ground as in the case of class 7–8 trucks. Understanding the impact of sound barriers on emission released from trucks with upward aligned exhaust tips requires further investigation. Since these emissions are released as an elevated source, it is possible that the inclusion of SBs trap these emissions in the cavity downwind of the roadway. Hence, ground level concentrations in residential communities nearby might increase as compared to the case where there is no SB. In 1998, California Air Resources Board identified particulate matter (PM) emissions from diesel–fueled engines as a toxic air contaminant. With the adoption of the on-road heavy-duty diesel vehicles (in-use) regulation in 2008, it is anticipated that diesel $PM_{2.5}$ emissions will be reduced by 50% from anticipated levels between 2015 and 2023 as compared to a scenario without the rule in place (http://www.arb.ca.gov/regact/2010/truckbus10/truckbusappg.pdf). Although the implementation of this regulation can significantly reduce near-roadway exposure to diesel exhaust PM, more health-protection strategies are required. This paper supports the deployment of sound walls as a strategy to reduce the exposures to emissions from cars; however, it does not provide any insight on impact of the roadside structures on emissions released at 3–4 m above the roadway.

Acknowledgements

We would like to thank Brandn Gazzolo, Raul-Delga Delgadillo and Trent Nash for their help in preparing and executing experiments. This report was prepared as a result of work sponsored in part by the South Coast Air Quality Management District (AQMD). The opinions, findings, conclusions, and recommendations are those of the authors and do not necessarily represent the views of AQMD. AQMD, its officers, employees, contractors, and subcontractors make no warranty, expressed or implied, and assume no legal liability for the information in this report. AQMD has not approved or disapproved this report, nor has AQMD passed upon the accuracy or adequacy of the information contained herein.

References

Addepalli, B., Pardyjak, E.R., 2013. Investigation of the flow structure in step-up street canyons—mean flow and turbulence statistics. Bound.-Lay. Meteorol. 148 (1), 133–155.
Adrian, R.J., 1988. Review of particle image velocimetry research. In: The Symposium on Optical Methods in Flow and Particle Diagnostics, 6th International Congress on Applications of Lasers and Electro-Optics. Optics and Lasers in Engineering, San Diego, CA, pp. 317–319, vol. 9.
Adrian, R.J., 1991. Particle-imaging techniques for experimental fluid-mechanics. Ann. Rev. Fluid Mech. 23, 261–304.
Adrian, R.J., 1997. Dynamic ranges of velocity and spatial resolution of particle image velocimetry. Meas. Sci. Technol. 8 (12), 1393–1398.
Baldauf, R., Thomas, E., Khlystov, A., Isakov, V., Bowker, G., Long, T., Snow, R., 2008. Impacts of noise barriers on near-road air quality. Atmos. Environ. 42, 7502–7507.
Beckett, K.P., Freer-Smith, P.H., Taylor, G., 1998. Urban woodlands: their role in reducing the effects of particulate pollution. Environ. Pollut. 99, 347–360.
Bouvet, T., Loubet, B., Wilson, J.D., Tuzet, A., 2007. Filtering of windborne particles by a natural windbreak. Bound.-Lay. Meteorol. 123 (3), 481–509.
Bowker, G.E., Baldauf, R., Isakov, V., Khlystov, A., Petersen, A., 2007. The effects of roadside structures on the transport and dispersion of ultrafine particles from highways. Atmos. Environ. 41, 8128–8139.
Brantley, H.L., Hagler, G.S., Deshmukh, P.J., Baldauf, R.W., 2014. Field assessment of the effects of roadside vegetation on near-road black carbon and particulate matter. Sci. Total Environ. 468, 120–129.
Bussoti, F., Grossoni, P., Batistoni, P., Ferreti, M., Cenni, E., 1995. Preliminary studies on the ability of plant barriers to capture lead and cadmium of vehicular origin. Aerobiologia 11, 11–18.
Clawson, K.L., Eckman, R.M., Johnson, R.C., Carter, R.G., Finn, D., Rich, J.D., Hukari, N.F., Strong, T., Beard, S.A., Reese, B.R., 2009. Near Roadway Tracer Study (2008). NOAA Technical Memorandum OAR ARL-260. Air Resources Laboratory, Idaho Falls, Idaho.
Dockery, D.W., Pope, C.A., 1994. Acute respiratory effects of particulate air pollution. Annu. Rev. Publ. Health 15 (1), 107–132.
Edwards, J., Walters, S., Griffiths, R.K., 1994. Hospital admissions for asthma in preschool children: relationship to major roads in Birmingham, United Kingdom. Arch. Environ. Health 49, 223–227.
Fackrell, J.E., Pearce, J.E., 1981. Parameters Affecting Dispersion in the Near Wake of Buildings, Central Electricity Generating Board, Report RD/M/1179N81, Marchwood Engineering Laboratories, UK, pp. 41.
Finn, D., Clawson, K.L., Carter, R.G., Rich, J.D., Eckman, R.M., Perry, S.G., Isakov, V., Heist, D.K., 2010. Tracer studies to characterize the effects of roadside noise barriers on near-road pollutant dispersion under varying atmospheric stability conditions. Atmos. Environ. http://dx.doi.org/10.1016/j.atmosenv.2009.10.012.
Guilbault, G.G., 1973. Practical Fluorescence: Theory, Methods and Techniques. Dekker, New York.
Halitsky, J., 1968. Gas diffusion near buildings. In: Slade, D.H. (ed.), TID-24190, Meteorol. and Atomic Energy, chapter 5–5, pp. 221–231.
Harrison, R.M., Leung, P.L., Somerville, L., 1999. Analysis of incidence of childhood cancer in the West Midlands of the United Kingdom in relation to the proximity of main roads and petrol stations. J. Occup. Environ. Med. 56, 774–780.
Heist, D.K., Perry, S.G., Brixey, L.A., 2009. A wind tunnel study of the effect of roadway configurations on the dispersion of traffic-related pollution. Atmos. Environ. 43, 5101–5111.
Houston, D., Ong, P.M., Wu, J., Winer, A., 2006. Proximity of licensed childcare to near-roadway vehicle pollution. Am. J. Public Health 96 (9), 1611–1617.
Jerrett, M., Burnett, R., Pope, C.A., Krewski, D., Newbold, K.B., Thurston, G., Shi, Y., Finkelstein, N., Calle, E.E., Thun, M.J., 2005. Spatial analysis of air pollution and mortality in Los Angeles. Epidemiology 16, 727–736.
Mao, Y., Wilson, J.D., Kort, J., 2013. Effects of a shelterbelt on road dust dispersion. Atmos. Environ. 79, 590–598.

McConnell, R., Berhane, K., Yao, L., Jerrett, M., Lurmann, F., Gilliland, F., Kuenzli, N., Gauderman, J., Avol, E., Thomas, D., Peters, J., 2006. Traffic, susceptibility, and childhood asthma. Environ. Health. Perspect. 114 (5), 766–772.
Pardyjak, E.R., Speckart, S.O., Yin, F., Veranth, J.M., 2008. Near source deposition of vehicle generated fugitive dust on vegetation and buildings: model development and theory. Atmos. Environ. 42 (26), 6442–6452.
Peters, A., Von Klot, S., Heier, M., Trentinaglia, I., Hormann, A., Wichmann, E., Lowel, H., 2004. Exposure to traffic and the onset of myocardial infarction. New. Engl. J. Med. 351, 1721–1730.
Pournazeri S., Pan H., Pellereau E., Princevac M., 2010. Localized effect of building height on street level flows and concentration: Water channel modeling. In: 90th AMS Annual Meeting, 16th Conference on Air Pollution Meteorology, 1, Atlanta, GA, January 2010.
Pournazeri, S., Princevac, M., Venkatram, A., 2012a. Rise of buoyant emissions from low-level sources in the presence of upstream and downstream obstacles. Bound.-Lay. Meteorol. 144 (2), 287–308. http://dx.doi.org/10.1007/s10546-012-9717-6.
Pournazeri, S., Princevac, M., Venkatram, A., 2012b. Scaling of building affected plume rise and dispersion in water channels and wind tunnels—Revisit of an old problem. J. Wind. Eng. Ind. Aerod. 2012. http://dx.doi.org/10.1016/j.jweia..01.00.
Pournazeri, S., Schulte, N., Si, T., Princevac, M., Venkatram, A., 2013. Dispersion of buoyant emissions from low level sources in urban areas: water channel modeling. Int. J. Environ. Pollut. 52 (3), 119–140. http://dx.doi.org/10.1504/IJEP.2013.058460.
Prasad, A.K., Adrian, R.J., Landreth, C.C., Offutt, P.W., 1992. Effect of resolution on the speed and accuracy of particle image velocimetry interrogation. Exp. Fluids 13 (2–3), 105–116.
Princevac, M., Baik, J.J., Li, X., Pan, H., Park, S.B., 2010. Lateral channeling within rectangular arrays of cubical obstacles. J. Wind. Eng. Ind. Aerod. http://dx.doi.org/10.1016/j.jweia.2009.11.001.
Snyder, W.H., 1972. Similarity criteria for the application of fluid models to the study of air pollution meteorology. Bound.-Lay. Meteorol. 3, 113.
Snyder, W.H., 1981. Guidelines for fluid modeling of atmospheric diffusion, EPA-600/8-81-009.
Snyder, W.H., Lawson R.E., 1994. Wind-tunnel measurements of flow fields in the vicinity of buildings. In: AMS, 8th Joint Conf. on Applic. of Air Poll. Meteor. with AWMA, Nashville, TN, Jan. 23–28.
Speckart, S.O., Pardyjak, E.R., 2014. A method for rapidly computing windbreak flow field variables. J. Wind. Eng. Ind. Aerod. 132, 101–108.
Steffens, J.T., Heist, D.K., Perry, S.G., Zhang, K.M., 2013. Modeling the effects of a solid barrier on pollutant dispersion under various atmospheric stability conditions. Atmos. Environ. 69, 76–85.
Veranth, J.M., Pardyjak, E.R., Seshadri, G., 2003. Vehicle-generated fugitive dust transport: analytic models and field study. Atmos. Environ. 37 (16), 2295–2303.
Wilhelm, M., Ritz, B., 2003. Residential proximity to traffic and adverse birth outcomes in Los Angeles County, California, 1994–1996. Environ. Health Perspect. 111, 207–216.
Yee, E., Gailis, R.M., Hill, A., Hilderman, T., Kiel, D., 2006. Comparison of wind-tunnel and water-channel simulations of plume dispersion through a large array of obstacles with a scaled field experiment. Bound.-Lay. Meteorol. 121, 389–432.